Revista Mexicana de Astronomía y Astrofísica, **42**, 117–126 (2006)

THE N(H_2)/I(CO) CONVERSION FACTOR: A TREATMENT THAT INCLUDES RADIATIVE TRANSFER

W. F. Wall

Instituto Nacional de Astrofísica, Óptica y Electrónica
Tonantzintla, Puebla, México

Received 2005 December 1; accepted 2006 February 7

RESUMEN

Se presenta un tratamiento que explica mejor el factor de conversión N(H_2)/I(CO) y que incluye la transferencia radiativa. A primera vista, incluir la transferencia radiativa parece superfluo para una línea ópticamente gruesa como CO J = 1 → 0. No obstante, dado que el medio interestelar es inhomogéneo, los fragmentos de gas (es decir, grumos) todavía pueden ser ópticamente delgadas hacia sus bordes y en las alas de los pérfiles de la línea. El tratamiento estadístico de Martin et al. (1984) de la transferencia radiativa a través una nube molecular con grumos se usa para derivar una expresión para el factor de conversión que supera los defectos de las explicaciones más tradicionales basadas en Dickman et al. (1986). Por un lado, el tratamiento presentado aquí posiblemente representa un avance importante al entender el factor de conversión N(H_2)/I(CO) pero, por otro lado, tiene sus propios defectos, que son discutidos aquí brevemente.

ABSTRACT

A treatment that better explains the N(H_2)/I(CO) conversion factor is given that includes radiative transfer. At first glance, involving radiative transfer seems superfluous for an optically thick line such as CO J = 1 → 0 line. However, given that the interstellar medium is inhomogeneous, the individual gas fragments (i.e., clumps) can still be optically thin toward their edges and in the wings of their line profiles. The statistical treatment by Martin et al.(1984) of the radiative transfer through a clumpy molecular cloud is used to derive an expression for the conversion factor that overcomes the shortcomings in the more traditional explanations based on Dickman et al. (1986). While possibly representing important step forward in understanding the N(H_2)/I(CO) conversion factor, the treatment here also has shortcomings of its own that are briefly discussed.

Key Words: **ISM: MOLECULES — ISM: DUST — ISM: ORION**

1. INTRODUCTION

In studies of the interstellar medium (ISM) the amount of gas and dust affects the physical mechanisms of the ISM and can affect the evolution of an entire galaxy. In particular, the amount of molecular gas in a cloud, cloud complex, spiral arm, or galaxy constrains the number of stars that form and the way that they form. The usual molecule for estimating molecular gas masses has been, and still is, CO (e.g., see IAU Symp. #170, 1997, and references therein). Specifically, observations of the J = 1 → 0 rotational line of the isotopologue, $^{12}C^{16}O$ (just CO for short), permit simple, but crude, estimates of the mass of molecular hydrogen in an astronomical source. The velocity-integrated brightness, I(CO), often called the *integrated intensity*, is multiplied by a standard conversion factor, N(H_2)/I(CO), to yield the molecular hydrogen column density, N(H_2), which gives the H_2 mass of the source after integrating over the source's projected area. The most current value of this conversion factor is about $2 \times 10^{20}\,\mathrm{H_2\,cm^{-2} \cdot (K \cdot km \cdot s^{-1})^{-1}}$ for the molecular gas in the disk of our Galaxy (Dame, Hartmann, & Thaddeus 2001). Why the CO J = 1 → 0 line should yield an estimate of column density is far from clear. As is well known (e.g., see Evans 1980; Kutner 1984; Evans 1999), the CO J = 1 → 0 line is optically

thick, obfuscating any simple explanation as to why it should probe molecular gas column densities.

Other tracers of molecular gas mass exist, tracers that do not possess the serious uncertainties posed by CO J = 1 → 0. While potentially simpler to use for determining column densities, the optically thin lines of the isotopologues $^{13}C^{16}O$ and $^{12}C^{18}O$ (just ^{13}CO and $C^{18}O$ in short form) are normally factors of about 3 to 50 weaker than the CO J = 1 → 0 line (e.g., Kutner 1984; Langer & Penzias 1990; Nagahama et al. 1998; Maddalena et al. 1986); the ^{12}CO lines are better for mapping large areas of molecular gas or for detecting weak sources, such as high-redshift galaxies (e.g., Brown & Vanden Bout 1992; Barvainis et al. 1997,1998; Alloin, Barvainis, & Guilloteau 2000; Carilli et al. 2002a). This makes the J = 1 → 0 line of CO, and the $N(H_2)/I(CO)$ factor, more useful or even essential in estimating the total molecular gas mass in some sources, resulting in a strong incentive for understanding the $N(H_2)/I(CO)$ factor's behavior.

The usual attempts at accounting for why the $N(H_2)/I(CO)$ factor, or X-factor, is relatively constant on multi-parsec scales are variations of the explanation given by Dickman et al. (1986), hereafter DSS86 (e.g., Sakamoto 1996). A summary of the DSS86 explanation follows. If T_R is the peak radiation temperature of the CO J = 1 → 0 line and Δv is the appropriately defined velocity width of this line, then $I(CO) = T_R \Delta v$. If the molecular gas under observation is virialized, then the observed velocity width is related to the mass of this gas and, therefore, to the gas column density averaged over the solid angle subtended by the observed gas. It was then easy to show that $N(H_2)/I(CO) \propto n^{0.5}/T_R$. The n was the gas density *averaged over the virialized volume of gas.* DSS86 found that n had to be $\sim few \times 10^2\,H_2\,cm^{-3}$ to give the observed value of $N(H_2)/I(CO)$; therefore it was assumed that this volume included entire clouds. Even if the gas does not fill the beam (a point to which we will return later), we would have T_R roughly proportional to the gas kinetic temperature, T_K, and we would still have $N(H_2)/I(CO) \propto n^{0.5}/T_K$. It is argued that the quantity $n^{0.5}/T_K$ does not strongly vary on multi-parsec scales, especially due to the weak dependence on density, resulting in a fairly stable value of X. Observational evidence does indeed seem to support a roughly constant value of the X-factor to within a factor of about 2 for the disk of our Galaxy, where $X \simeq 2 \times 10^{20}\,cm^{-2} \cdot (K \cdot km \cdot s^{-1})^{-1}$ (see, e.g., Dame et al. 2001; Strong et al. 1988, and references therein), although the observations of Sodroski et al. (1994) and Strong et al. (2004) suggest a higher value of X in the outer disk (a claim that is at odds with Carpenter, Snell, & Schloerb 1990). The values of the X-factor that apply to the disks of other spiral galaxies are often within factors of about 3 of that of the Galactic disk X-factor (e.g., Young & Scoville 1982; Adler et al. 1992; Guélin et al. 1995; Nakai & Kuno 1995; Brouillet et al. 1998; Rand, Lord, & Higdon 1999; Meier, Turner, & Hurt 2000; Meier & Turner 2001; Boselli, Lequeux, & Gavazzi 2002; Rosolowski et al. 2003). The goals of the current paper are to address the deficiencies of the DSS86 explanation of the X-factor and improving upon this explanation. Improvements are necessary because DSS86 has the following problems:

1. *No treatment of radiative transfer.* This is a fundamental problem with DSS86. At first glance, it might seem superfluous to treat radiative transfer in the optically thick case. However, if we consider a clumpy medium, where the clumps can have optically thin edges and optically thin frequencies in their line profiles, then treating radiative transfer is essential for understanding the X-factor. In particular, *the optically thin limit of CO J = 1 → 0 must also be included.* Any *complete* treatment must include the optically thin case, whether this case is observed in nature or not. This case cannot be included easily in the DSS86 explanation because it includes the virial theorem *without* including radiative transfer —virialization by itself says nothing about the optical depth of the emission.

2. *Sensitivity to T_K and $n(H_2)$.* As discussed in Wall (2006), I(CO) and the X-factor estimate the molecular hydrogen column densities to within factors of about 2 of the values obtained from optically thin tracers for the majority of positions in the Orion clouds. In general, we know that molecular cloud kinetic temperatures and densities have a full range of an order of magnitude on multi-parsec scales (cf. Sanders, Scoville, & Solomon 1985; Sakamoto et al. 1994; Helfer & Blitz 1997; Plume et al. 2000). Since the X-factor supposedly varies as $n^{0.5}/T_K$, the temperature and density variations can *each* change X by factors of 3 to 10 (unless $n^{0.5}$ were to vary like T_K, but this is unlikely to be true in general, especially if there is pressure equilibrium). Thus the X of DSS86 is too sensitive to the density and kinetic temperature. Having a weaker dependence of X on n and T_K,

like X $\propto (n/\mathrm{T_K})^{0.3}$, would resolve this sensitivity problem; variations of an order of magnitude in either n or $\mathrm{T_K}$ would allow X to vary by less than a factor of 2.

3. *Virialization of entire clouds.* DSS86 require low densities (i.e., n(H_2) $\sim few \times 10^2\,\mathrm{cm^{-3}}$) to obtain the observed value of the X-factor. Given that the critical density of the CO J = 1 → 0 transition is $\sim 3\times10^3\,H_2\,\mathrm{cm^{-3}}$, the densities of the CO-emitting structures are about an order of magnitude higher (also see the average densities of the filaments found by Nagahama et al. 1998).

4. *Stronger dependence of peak T_R on N(H_2) than of* Δv *on N(H_2) is not explained.* DSS86 require that the observed velocity width of the line depends on the gas column density. However, there is evidence that it is the peak radiation temperature, $\mathrm{T_R}$, that depends on N(H_2) and that Δv has only a weak dependence on N(H_2) (see Wall 2006; Heyer, Carpenter, & Ladd 1996).

The purpose of the current paper is to propose an improved approach for understanding the X-factor that will resolve, or at least mitigate, the problems with DSS86. For example, the explanation proposed here includes radiative transfer in a clumpy medium and shows how the optically thick CO J = 1 → 0 emission of a cloud can be sensitive to the optical depths of the individual clumps. As a result, this explanation will permit, in some circumstances, a very weak dependence on $\mathrm{T_K}$ and n(H_2). Also, even though we will also use the virial theorem (in its simplest form), we can apply it to scales smaller than entire clouds. And the X-factor in the current proposed explanation will lose its dependence on the virial theorem in the optically thin case. In addition, the proposed approach will naturally explain the dependence of the peak $\mathrm{T_R}$ on N(H_2). This improved approach has shortcomings of its own, but nevertheless may represent an important step forward in understanding the X-factor.

2. A FORMULATION FOR THE X-FACTOR

2.1. *Radiative Transfer in a Clumpy Cloud*

The X-factor may yield a reasonable estimate of the molecular gas column density, because the integrated intensity of the CO J = 1 → 0 line is essentially counting optically thick clumps in the gas in the beam (e.g., see Evans 1999). This explanation does not, by itself, directly relate the masses of individual clumps to the observed integrated intensity, because, again, the clumps are optically thick in the CO J = 1 → 0 line. Applying *only* the DSS86 approach to the clumps will not work, because, as discussed in the introduction, DSS86 and the observed value of the X-factor together require densities an order of magnitude lower than those found in the clumps of real clouds. The DSS86 derivation of the X-factor depends on the beam-averaged column density, N, and the observed velocity width, Δv. We need a treatment of the problem in which the beam-averaged quantities, N and Δv, are cancelled out in favor of the corresponding quantities for an individual clump, i.e., N_c and $\Delta \mathrm{v_c}$. And we need a treatment of the radiative transfer in a clumpy medium. Martin et al. (1984) (hereafter MSH84) developed a method for describing radiative transfer through a clumpy medium in a highly simplified case: they assumed that each clump was homogeneous and in LTE. For additional simplicity, they also assumed that the clumps were identical, although they pointed out that their method could be easily generalized to clumps with a spectrum of properties (see the Appendix of MSH84). The assumption of LTE was necessary because the implicit assumption is that the excitation temperature *of the transition* is constant throughout each clump, which is easily attained if the density is high enough for LTE. This assumption is particularly appropriate for the CO J = 1 → 0 line: because of its high optical depth (i.e., $\tau \sim$ *few*) and low critical density (i.e., $n_{crit} \simeq 3\times10^3\,\mathrm{cm^{-3}}$), this line is largely thermalized (i.e., close to LTE). Hence the method of MSH84 is appropriate here.

MSH84 used a statistical approach to find the appropriately averaged optical depth on a sightline through a cloud with clumps in a vacuum. The effective optical depth on a given sightline was expressed in terms of the individual clump opacities and the mean number of clumps on a sightline with velocities within a clump's velocity width for the case of identical clumps. This effective optical depth is the expectation value of the total optical depth of the clumps on a given sightline. Computing this expectation value then depends on an average opacity over all impact parameters for each clump. The appropriate average is the average over values of $[1-\exp(-\tau)]$ and, accordingly, the effective optical depth, τ_{ef}, is given by $1-\exp(-\tau_{ef}) = \langle 1-\exp(-\tau)\rangle$, which implies $\exp(-\tau_{ef}) = \langle \exp(-\tau)\rangle$, where $\langle\rangle$ indicates expectation value. In the approximation of the spectral line width, Δv, being much larger than the velocity width of an individual clump, $\Delta \mathrm{v_c}$, τ_{ef} can be ex-

pressed as the product of the number of clumps per clump velocity width on a sightline and the effective optical depth of an individual clump. If N is the beam-averaged gas column density and N_c is the gas column density averaged over the projected area of a single clump, then $(N/N_c)(\Delta v_c/\Delta v)$ is the number of clumps per sightline averaged over the beam per clump velocity width at the line central velocity. (Note that, below, N_c is actually the column density on the central sightline through the clump, but this change in definition accords with the definition of the clump average optical depth.) If τ_0 is the optical depth on a sightline through the center of a single clump, then, following MSH84, $A(\tau_0)$ is the clump effective optical depth. (Note that MSH84 called $A(\tau_0)$ the effective optically thick area of the clump. Even though their term is more accurate, the simpler "clump effective optical depth" is adopted here.) Consequently,

$$\tau_{ef}(v_z) = \frac{N}{N_c}\frac{\Delta v_c}{\Delta v}\, A(\tau_0) \exp\left(-\frac{{v_z}^2}{2\,\Delta v^2}\right) \quad , \qquad (1)$$

where v_z is the velocity component along the sightline and where a Gaussian line profile has been assumed. If $\tau(x,y)$ is the clump optical depth on the sightline at position (x,y) with respect to a sightline through the clump center, then the clump effective optical depth is given by

$$A(\tau_0) \;= \frac{1}{\sqrt{2\pi}\;\Delta v_c\; a_{_{eff}}} \int dv \int dx \int dy \cdot \cdot \left\{1 - \exp\left[-\tau(x,y)\,\exp\left(-\frac{v^2}{2\,\Delta v_c^2}\right)\right]\right\}, \qquad (2)$$

where $a_{_{eff}}$ is clump's effective projected area defined in terms of its optical depth:

$$a_{_{eff}} \equiv \frac{1}{\tau_0}\int dx \int dy\; \tau(x,y) \quad . \qquad (3)$$

The τ_0 is simply $\tau(x=0, y=0)$, the optical depth through the clump's center and at the center of the clump's velocity profile. The integrals in both (2) and (3) are over the projected area of the clump and over the clump's velocity profile. Note that, in general, the expression for $\tau_{ef}(v_z)$ would have integrals over both the line spectral distribution (over v_z) and over the velocity distribution of each individual clump (over v). But, as done in MSH84, we assume that Δv is significantly larger than Δv_c and all clumps are assumed to be identical. This then leads to expressions (1) and (2). Numerically integrating equation (2) gives Figure 1, which shows the variation of $A(\tau_0)$ as a function of τ_0 for two types of clumps: cylindrical (seen orthogonally to the axis of symmetry) and spherical.

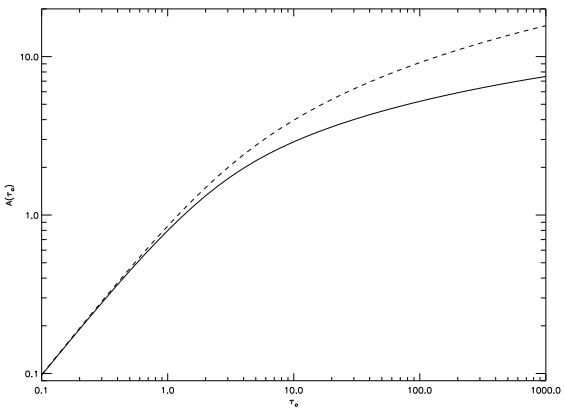

Fig. 1. The effective optical depth of a clump, $A(\tau_0)$, after averaging over its projected area is plotted against the optical depth through the clump center, τ_0. The solid curve shows $A(\tau_0)$ versus τ_0 for a cylindrical clump viewed perpendicularly to the symmetry axis. The optical depth profile across the cylinder, from the central axis towards the edges, is Gaussian. The dashed curve shows the corresponding curve for a spherical clump. The optical depth profile from the sphere's center towards the edges is also Gaussian. The Gaussian spherical clump case was also treated and plotted in MSH84.

The observed line radiation temperature, T_R, is then related to τ_{ef} by the usual expression

$$T_R(\nu) = \mathcal{J}_\nu(T_K)\;\left[1 - \exp(-\tau_{ef})\right] \quad . \qquad (4)$$

T_K is the gas kinetic temperature. As stated earlier, LTE is assumed for the emission of the spectral line at frequency ν. The $\mathcal{J}_\nu(T_K)$ is correction for the failure of the Rayleigh-Jeans approximation and for the cosmic microwave background emission. Of course when $\tau_{ef} \ll 1$, we have the simplified form of Eq. (4):

$$T_R(\nu) = \mathcal{J}_\nu(T_K)\,\tau_{ef} \quad . \qquad (5)$$

This is often called the "optically thin limit" for the equation of radiative transfer. An important point here is that the effective optical depth is in the optically thin limit *even though the individual clumps can still be quite optically thick.* And this, of course, will provide a partial explanation for the X-factor. Substituting Eq. (1) into Eq. (5) yields

$$T_R(v_z) = \mathcal{J}_\nu(T_K)\,\frac{N}{N_c}\frac{\Delta v_c}{\Delta v}\, A(\tau_0) \exp\left(-\frac{{v_z}^2}{2\,\Delta v^2}\right) \quad . \qquad (6)$$

As mentioned previously, the quantity $(\mathrm{N/N_c})(\Delta \mathrm{v_c}/\Delta \mathrm{v})$ is the number of clumps per sightline averaged over the beam within a clump velocity width at the line central velocity. This quantity can be much less than unity, thereby permitting $\tau_{ef} \ll 1$ even for $\mathrm{A}(\tau_0) \gg 1$. (When $(\mathrm{N/N_c})(\Delta \mathrm{v_c}/\Delta \mathrm{v}) < 1$, it is similar to the geometric area filling factor within a narrow velocity interval, although it is not *necessarily* equivalent.) Since $\mathrm{A}(\tau_0)$ is roughly equivalent to $[1 - \exp(-\tau)]$ for a single clump, the meaning of expression (6) is clear: it is the specific intensity of a single clump at velocity v_z — $\sim \mathcal{J}_\nu(\mathrm{T_K})\,[1-\exp(-\tau)]$ —multiplied by the number of clumps at that velocity within a clump velocity width— $(\mathrm{N/N_c})(\Delta \mathrm{v_c}/\Delta \mathrm{v}) \exp[-{v_z}^2/(2\,\Delta \mathrm{v}^2)]$. Simply multiplying the intensity of a single clump by the number of clumps gives the observed intensity *if* the clumps are radiatively de-coupled, and this is ensured if $\tau_{ef} \ll 1$. As τ_{ef} increases and becomes optically thick, the different clumps within each velocity interval start absorbing each other's emission and the radiation temperature approaches the source function $\mathcal{J}_\nu(\mathrm{T_K})$ asymptotically.

We can now better understand the behavior of the curves in Fig. 1. $\mathrm{A}(\tau_0)$ represents the level of emission from a single clump averaged over the clump's projected area. When $\tau_0 \ll 1$, $\mathrm{A}(\tau_0) \simeq \tau_0$ because all lines of sight through the clump and the line's profile at all the clump's internal velocities are optically thin. As τ_0 increases past unity, $\mathrm{A}(\tau_0)$ continues growing because of those lines of sight and those velocities at which the emission is still optically thin. Fig. 1 shows two curves: one for a cylindrical clump of gas (i.e., a filament) and one for a spherical clump. The cylinder is viewed side-on (i.e. with its symmetry axis perpendicular to the sightline) and has length h. If the symmetry axis is the x-axis, then a Gaussian variation of the optical depth with y was adopted:

$$\tau(x,y) = \tau_0 \exp\left(-\pi h^2 \frac{y^2}{{a_{_{eff}}}^2}\right) \quad . \tag{7}$$

The spherical clump also has Gaussian spatial variation with optical depth, but with radial distance, p, from the central sightline through the clump:

$$\tau(x,y) = \tau_0 \exp\left(-\pi \frac{p^2}{a_{_{eff}}}\right) \quad , \tag{8}$$

where $p = \sqrt{x^2+y^2}$. This case was also treated by MSH84, and it is included here for comparison. (Note that the $a_{_{eff}}$ used here corresponds to the r_o^2 of MSH84.) The effective optical depth of the spherical clump grows faster with τ_0 for $\tau_0 \gtrsim 1$ than that of the cylindrical clump because the former's optically thick area is growing simultaneously in two dimensions, whereas the latter's grows only in one. While $\mathrm{A}(\tau_0)$ can grow without bound in these idealized cases, $\mathrm{T_R}$ cannot. Eventually, $\mathrm{A}(\tau_0)$ will grow large enough that $\tau_{ef} \ll 1$ is no longer valid and $\mathrm{T_R}$ asymptotically approaches $\mathcal{J}_\nu(\mathrm{T_K})$. The growing τ_0 causes this to happen because the clumps start crowding each other spatially and in velocity, due to their increasing optically thick areas and their increasingly saturated line profiles.

The curves of Fig. 1 demonstrate that we can represent them as power-laws in τ_0 for $\tau_0 \leq 1$ or $\tau_0 \geq 3$:

$$\mathrm{A}(\tau_0) \simeq \mathrm{k_A}\,\tau_0^{\epsilon} \quad . \tag{9}$$

The values of k_A and ϵ obviously depend on the specific $\tau(x,y)$ —the opacity structure of the clump, except in the optically thin case. When $\tau_0 < 1$, we have $k_A = 1$ and $\epsilon = 1$, regardless of the specific variation of $\tau(x,y)$. Except for the optically thin case, a lower value of ϵ, i.e., closer to zero, indicates a clump with a better defined outer edge, like a hard sphere. Conversely, a higher value of ϵ, i.e., closer to unity, indicates a clump with a more tenuous, or fluffier, outer region. Accordingly, ϵ will be called the "fluffiness" of the clump.

2.2. *Relating Clump Velocity Width with Column Density*

DSS86 required virialization in order to relate the line velocity width to the gas column density. That is also required here, but it will be combined with the radiative transfer in a clumpy cloud discussed in the previous subsection. The virial theorem in its simplest form neglects the effects of surface pressure and magnetic fields. Assuming a spherical clump of uniform density gives

$$\Delta \mathrm{v_c} \;=\; k_v\,\mathrm{N_c^{0.5}\,L_c^{0.5}} \quad , \tag{10}$$

and

$$k_v \;\equiv\; \left(\frac{\pi}{15}\,G\,\mu \mathrm{m_{H2}}\right)^{0.5} \quad . \tag{11}$$

Numerically in *cgs* units, this is

$$k_v \;=\; 2.47 \times 10^{-16} \quad ,$$

where μ is the correction for the mass of helium in the ISM and $\mu = 1.3$ was used. The $\mathrm{N_c}$ and L_c are the column density and path length through the clump central sightline, respectively. The $\mathrm{m_{H2}}$ is the mass of the hydrogen molecule.

2.3. *Relating Clump Optical Depth with Column Density*

The clump optical depth on the sightline through the clump's center, τ_0, can be written in terms of the column density of CO in level J, N_J:

$$N_{_J} = \frac{8\pi}{A_{_{J,J-1}}\lambda^3_{_{J,J-1}}} \times \times\left[\exp\left(\frac{T_{_{J,J-1}}}{T_{_K}}\right)-1\right]^{-1} \tau_0\sqrt{2\pi}\Delta \mathrm{v_c} \quad . (12)$$

This comes from Eq. (A9) of Wall (2006) after applying the Boltzmann factor to change N_{J-1} to N_J. The velocity integral was replaced by $\tau_0\sqrt{2\pi}\Delta \mathrm{v_c}$, where τ_0 is the optical depth at the center of the clump's velocity profile and on the sightline through the clump's center. $T_{_{J,J-1}}$ is the energy of the $J \rightarrow J-1$ transition in units of temperature: i.e., $T_{_{J,J-1}} = h\,\nu_{_{J,J-1}}/k$ with $\nu_{_{J,J-1}}$ as the frequency of the transition. $A_{_{J,J-1}}$ and $\lambda_{_{J,J-1}}$ are the spontaneous transition rate and the wavelength of the transition, respectively. LTE is assumed, so $\mathrm{T_K}$ applies in place of $\mathrm{T_X(J \rightarrow J-1)}$. We can determine the total column density of CO, $N(CO)$, by substituting Eq. (12) into Eq. (A22) of Wall (2006) and rearranging:

$$\tau_0 = \frac{3A_{10}\lambda^3_{10}}{8\sqrt{2}\,\pi^{\frac{3}{2}}\Delta \mathrm{v_c} \mathrm{Q(T_K)}} \times \times\left[1-\exp\left(-\frac{T_{10}}{T_{_K}}\right)\right]\mathrm{N_c}X(\mathrm{CO}) \quad . \quad (13)$$

where $Q(T_{_K})$ is the partition function of CO and J was set to 1. The $N(\mathrm{CO})$ was replaced by $\mathrm{N_c}X(\mathrm{CO})$, where $X(\mathrm{CO})$ is the abundance of CO relative to H_2. The following values are used (see Wall 2006, and references therein): $A_{10} = 7.19 \times 10^{-8}\,\mathrm{s^{-1}}$, $T_{10} = 5.54\,\mathrm{K}$, $\lambda_{10} = 0.2601\,\mathrm{cm}$, and $X(\mathrm{CO}) = 8 \times 10^{-5}$. Accordingly,

$$\tau_0 = \frac{1.21 \times 10^{-14}}{\sqrt{2\pi}\Delta \mathrm{v_c} \mathrm{Q(T_K)}}\left[1-\exp\left(-\frac{5.54}{T_{_K}}\right)\right]\mathrm{N_c} \quad . \quad (14)$$

The above expression can be represented more simply as a power-law in $\mathrm{T_K}$:

$$\tau_0 = \frac{k_\tau}{\sqrt{2\pi}\Delta \mathrm{v_c}}\,\mathrm{N_c T_K^{-\gamma}} \quad . \quad (15)$$

The exact values of k_τ and γ depend on the temperature range and can be computed by numerically comparing expressions (15) and (14). In the high-temperature limit, however, an analytical solution is possible. This limit means that $\mathrm{T_K} \gg T_{10}$ and $Q(\mathrm{T_K}) \rightarrow 2\mathrm{T_K}/T_{10}$ and $[1-\exp(-T_{10}/T_{_K})] \rightarrow T_{10}/T_{_K}$. This results in $k_\tau = 1.85 \times 10^{-13}$ in *cgs* units and $\gamma = 2$. But we will be interested in the temperature range $\mathrm{T_K} = 10$ to $20\,\mathrm{K}$. The necessary numerical comparison gives us

$$k_\tau = 7.30 \times 10^{-14}\ (\textit{cgs}\ \text{units})$$

and

$$\gamma = 1.75\,,$$

for that range. This approximation is accurate to within 1–2% in the above specified range. Equation (15) simplifies further by using expression (10) for $\Delta \mathrm{v_c}$ and $n_c = \mathrm{N_c}/L_c$:

$$\tau_0 = \frac{k_\tau}{k_v\sqrt{2\pi}}\,n_c^{0.5}\mathrm{T_K^{-\gamma}} \quad . \quad (16)$$

This interesting result suggests that the optical depth for this simplified case (i.e., the velocity profile of the optical depth is a simple Gaussian) of a virialized clump does not explicitly depend on the sightline pathlength nor the velocity width, but on their ratio. This is related to the Sobolev approximation (e.g., see Shu 1991) in which the optical depth is dependent on the velocity gradient within a given region and not explicitly on the region's size. The pathlength-to-velocity-width ratio ($L_c/\Delta \mathrm{v_c}$) in a virialized clump is determined by the average density, the spatial variation of the density, and the geometry. Therefore, the optical depth depends on those things and the gas temperature, but with *no* dependence on the clump size or velocity width (at least for this simplified case).

2.4. *The X-Factor*

Understanding how to combine the results of the previous subsections to derive an expression for the X-factor requires examining the observational data that inspired the current paper in the first place. Figure 2 shows the Orion data discussed in Wall (2006): the peak radiation temperature of the ^{12}CO J = 1 → 0 line (i.e., $\mathrm{T_R}$) for various positions in the Orion clouds normalized to the source function at each position (i.e., $\mathcal{J}_\nu(\mathrm{T_K})$, the source function in temperature units) versus the gas column density (i.e., $\mathrm{N(H_2)}$) as determined from ^{13}CO J = 1 → 0. The plots demonstrate a clear correlation between $\mathrm{T_R}/\mathcal{J}_\nu(\mathrm{T_K})$ and $\mathrm{N(H_2)}$. The Spearman rank-order correlation test indicates that the correlation exists at better than the 99.99% confidence level. This is more than just the expected correlation between the

J = 1 → 0 lines of ^{12}CO and ^{13}CO, because the $\mathcal{J}_\nu(T_K)$ is determined from the dust temperature (see Wall 2006, for details). This suggests that the dust temperature really is a reliable measure of the kinetic temperature of the molecular gas, at least for the Orion clouds on the scales of parsecs (see Wall 2006,a,b, for more discussion of this). One way of explaining the correlation visible in Fig. 2 is that the area filling factor of the clump in each clump velocity interval is less than unity. A rising beam-averaged column density, N, means the filling factor is rising as more and more clumps fill the beam in each velocity interval. Obviously, the goal here is to be very specific about the relationship between $T_R/\mathcal{J}_\nu(T_K)$ and N(H_2). There is sufficient scatter and uncertainty in the data that it is not possible to rule out *a priori* a number of such relationships.

Nevertheless, from simple radiative transfer theory, we know that the specific intensity of a source normalized to its source function, usually written I_ν/S_ν, will vary like $1 - \exp(-\tau)$ when plotted against the optical depth through the source, τ. Given that the column density, N, is proportional to τ for constant kinetic temperature and density, the data in Fig. 2 mimic a curve with the form $1 - \exp(-aN)$ (see the plotted curves), where the aN probably represents some kind of optical depth. The majority of the data points are on the roughly linearly rising portion of the curve. This represents the optically thin region of the curve, *but the* ^{12}CO J = 1 → 0 *is known to be optically thick* from comparisons with the optically thin isotopologue ^{13}CO. Therefore, *a clue to understanding the X-factor is realizing that CO* J = 1 → 0 *emission behaves like it is optically thin, despite being optically thick.* This apparent contradiction is resolved when we consider the effective optical depth as described previously. While the individual clumps are themselves optically thick in CO J = 1 → 0, the cloud is optically thin "to the clumps." In other words, the emission from every clump in the telescope's beam through the cloud reaches the observer. An analogy would be observing the H I 21 cm line from an atomic cloud. In this case, the cloud is optically thin "to the atoms" in the sense that the emission from every atom in the telescope's beam through the cloud reaches the observer. And since every hydrogen atom is nearly identical in its 21 cm line emission properties, the conversion from I(H I) to N(H I) is physically straightforward and undisputed. For converting from I(CO) to N(H_2), assuming absolutely identical clumps would give a constant value of the X-factor, relatable to the clumps' properties. But

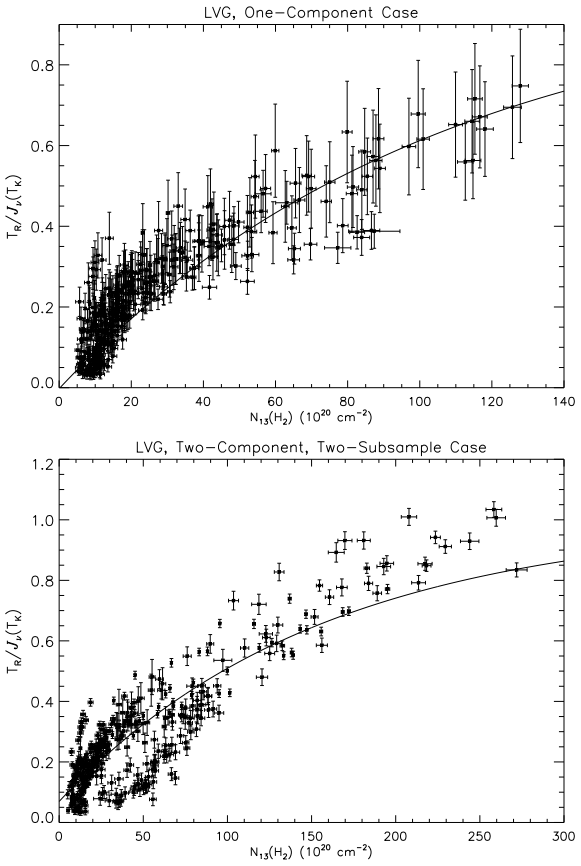

Fig. 2. Plots of the CO J = 1 → 0 line radiation temperature, T_R, normalized to its source function, $\mathcal{J}_\nu(T_K)$, versus the ^{13}CO J = 1 → 0 derived H_2 column density. Both plots are reproduced from Wall (2006). The curves are of the form $y = 1 - exp(-a\,x - b)$, where, in the ideal case, $b = 0$. The upper plot is for the LVG, one-component models of Wall (2006) and the lower plot is for the LVG, two-component, two-subsample models of that paper. (The source function for the two-component models is the effective source function as defined in Wall 2006). Given that x is in units of $10^{20}\,H_2\,cm^{-2}$, $a = (9.5\pm0.4)\times10^{-3}$ and $b = (2.4\pm5.5)\times10^{-3}$ for the upper plot and $a = (6.4\pm0.2)\times10^{-3}$ and $b = (7.2\pm0.8)\times10^{-2}$ for the lower plot.

we need not restrict the clump properties so severely to explain the X-factor. All we need is to have the clumps similar *on average* from one beam to the next for the X-factor to stay relatively constant.

We now need to quantify this picture, so that we might better understand it and its limitations. As Fig. 2 clearly shows, the $T_R/\mathcal{J}_\nu(T_K) \propto N$ for $N \lesssim 1$ to $2 \times 10^{22}\,H_2\,cm^{-2}$. This is in the $\tau_{ef} \ll 1$ limit, so Eq. (6) applies and it has the desired proportionality. Of course, this proportionality is only visible if the clump properties —N_c, Δv_c, and

$A(\tau_0)$— and the observed line width, Δv, do not vary strongly with N. In fact, the scatter visible in the plots of Fig. 2 is probably due to variations in all four of these quantities. Integrating Eq. (6) over velocity, v_z, gives

$$\begin{aligned} I(CO) &= \sqrt{2\pi}\, T_R(0)\, \Delta v\,, \\ &= \sqrt{2\pi}\, \mathcal{J}_\nu(T_K)\tau_{ef}(0)\, \Delta v \quad . \end{aligned} \tag{17}$$

$T_R(0)$ is the radiation temperature of the CO J = $1 \rightarrow 0$ line at $v_z = 0$ and is also the peak radiation temperature of this line. Similarly, $\tau_{ef}(0)$ is the effective optical depth at $v_z = 0$. The X-factor is then given by

$$X_f = \left[\sqrt{2\pi}\, \mathcal{J}_\nu(T_K)\, \tau_{ef}(0)\, \Delta v\, N^{-1}\right]^{-1} . \tag{18}$$

If we now substitute Eq. (1) evaluated at $v_z = 0$ into the above, then

$$X_f = \left[\sqrt{2\pi}\, \mathcal{J}_\nu(T_K)\, A(\tau_0)\, \Delta v_c\, N_c^{-1}\right]^{-1} . \tag{19}$$

The important thing to notice here is that the directly observed quantities, N and Δv, have been replaced by the corresponding clump properties, N_c and Δv_c. In fact, all the parameters in expression (19) are clump parameters, as desired. It is convenient to define

$$C_T \equiv \frac{T_K}{\mathcal{J}_\nu(T_K)} \quad . \tag{20}$$

We now use the approximation $\mathcal{J}_\nu(T_K) \simeq T_K - 3.4\,K$ for $T_K \gtrsim 10\,K$ and the frequency of the ^{12}CO J = $1 \rightarrow 0$ line, $\nu = 115.271\,GHz$. This is good to within 0.4% of T_K (and within 0.6% of $\mathcal{J}_\nu(T_K)$). Consequently,

$$C_T = \frac{T_K}{T_K - 3.4\,K} \quad , \tag{21}$$

which approaches unity as T_K grows large. Now we substitute the results of the previous subsections into equation (19): equation (9) for $A(\tau_0)$, (16) for τ_0, (10) for Δv_c, and T_K/C_T for $\mathcal{J}_\nu(T_K)$. We also use $n_c = N_c/L_c$. These substitutions yield

$$X_f = (2\pi)^{\frac{1}{2}(\epsilon-1)}\, C_T\, k_A^{-1}\, k_\tau^{-\epsilon}\, k_v^{\epsilon-1}\, T_K^{\gamma\epsilon-1}\, n_c^{\frac{1}{2}(1-\epsilon)} \quad . \tag{22}$$

The above formulation for X_f obviously accomplishes the goal of insensitivity to the parameters T_K and n_c that we have sought for X_f. The fluffiness parameter, ϵ, is in the range 0 to 1; any value in that range that is greater than 0 will confer a greater *in*sensitivity than occurs for the DSS86 explanation. A particularly interesting example is that value of ϵ for which $\gamma\epsilon - 1 = 0$. In the high temperature limit, $C_T \rightarrow 1$ and $\gamma \rightarrow 2$ and, if $\epsilon = 0.5$, then X_f *has no dependence on temperature.* (Notice that the density dependence is also very weak in this case: $X_f \propto n_c^{0.25}$.) Given that the CO J = $1 \rightarrow 0$ line is optically thick, this is counterintuitive; raising the temperature by some factor should simply increase I(CO) by the same factor (in the high-T_K limit), thereby decreasing X_f by that factor. That is not the case here. Here we are dealing with a clumpy medium where the optical depth varies across the projected area of each clump. There will always be some sightlines through a clump that will still be optically thin. There will also be some velocities in the clump's spectral line profile where the line emission is still optically thin. As T_K increases, τ_0 goes like T_K^{-2}, so that $A(\tau_0)$ goes like T_K^{-1} (see Eqs (15) and (9). But $\mathcal{J}_\nu(T_K)$ goes like T_K^1 (in this high-T_K limit), meaning that the observed T_R stays constant. The effect of the increasing kinetic temperature of the gas is cancelled by the decreasing effective optical depth of the clumps. Another way of saying this is that the effect of the rising temperature is cancelled by the shrinking effective optically thick areas of the clumps; the filling factors of the clumps decline as the temperature rises. (Note that this special case also occurs for lower temperatures. For $T_K = 10$ to $20\,K$, for example, $C_T \propto T_K^{-0.34}$ and $\gamma = 1.75$. The value of ϵ for which X_f is independent of temperature would be 0.77.) Therefore, *despite the optical thickness of the spectral line in the emitting clumps, changing the optical depths of the individual clumps will still have an appreciable effect on the line strength.* And this will reduce the dependence of the X-factor on the temperature and the density of the gas within the clumps.

3. CONCLUSIONS

What this treatment means in the astronomical context will be examined in more detail in a future paper (i.e., Wall 2006c). For now, it can be stated that the goals set out in the introduction have been largely accomplished:

1. *Treatment of radiative transfer.* This is no longer a problem given that the treatment here explicitly included the optical depth of the emitting structures (i.e., clumps). The optically thin case is now implicitly included by simply setting the fluffiness to unity (i.e., $\epsilon = 1$). This gives the correct relationship between the column density and the integrated intensity for the optically thin case in LTE.

2. *Reduced Sensitivity to T_K and n(H_2).* As the example in the previous section illustrates, the sensitivity to clump density and temperature can be greatly reduced or even eliminated (for the case of T_K only). For the case of a spherical clump with a Gaussian spatial variation of the optical depth, this dependence is roughly, $X_f \propto (n_c/T_K)^{0.3}$.

3. *Virialization of entire clouds is not necessary.* By using densities more representative of individual clumps, i.e., $n_c \sim few \times 10^3\,cm^{-3}$, the treatment given here will yield X-factor values easily within factors of 2 of those observed in our Galaxy.

4. *Stronger dependence of peak T_R on N(H_2) than of Δv on N(H_2) is now explained.* Given that the X-factor in this treatment depends on the velocity width of the individual clumps and not on the observed velocity width, Δv, of all the gas in the beam, the lack of dependence on Δv is now explained.

However, despite these successes, problems still remain:

1. *Sensitivity to ϵ.* The previous sensitivity to the physical parameters of density and temperature has now been replaced by the strong dependence on yet another physical parameter: ϵ. Why this parameter should remain roughly constant is uncertain. Nevertheless, it's variation maybe one reason why the X-factor can be very different in certain special regions such as the Galactic Centre region (e.g., Sodroski et al. 1995; Dahmen et al. 1998).

2. *Clump optical depths too high.* Given reasonable temperatures and densities (i.e. $T_K \sim 10$–$20\,K$ and $n_c \sim few \times 10^3\,cm^{-3}$) for the clumps, the central sightline optical depths in the ^{12}CO J = 1 $\rightarrow$ 0 line are an order of magnitude higher than expected from observations of the optically thin ^{13}CO J = 1 $\rightarrow$ 0 line. However, the X-factor is only reasonably constant on the scales of many parsecs. On such scales, the central sightline optical, τ_0, is not really the relevant quantity; the average over the clump's projected area, A(τ_0), is the relevant quantity and is about an order of magnitude smaller.

A more detailed discussion of the problems will be given in Wall (2006c). Overall, the treatment holds much promise, given that it includes basic radiative transfer.

This work was supported by CONACyT grants #211290-5-0008PE and #202-PY.44676 to W. F. W. at INAOE. I am very grateful to W. T. Reach for his comments and support. I thank T. A. .D. Paglione, G. MacLeod, E. Vazquez Semadeni, and others for stimulating and useful discussions. The author is grateful to R. Maddalena and T. Dame, who supplied the map of the peak ^{12}CO J = 1 $\rightarrow$ 0 line strengths and provided important calibration information.

REFERENCES

Adler, D. S., Lo, K. Y., Wright, M. C. H., Rydbeck, G., Plante, R. L., & Allen, R. J. 1992, ApJ, 392, 497
Alloin, D., Barvainis, R., & Guilloteau, S. 2000, ApJ, 528, L81
Barvainis, R., Alloin, D., Guilloteau, S., & Antonucci, R. 1998, ApJ, 492, L13
Barvainis, R., Maloney, P. R., Antonucci, R., & Alloin, D. 1997, ApJ, 484, 695
Boselli, A., Lequeux, J., & Gavazzi, G. 2002, A&A, 384, 33
Brouillet, N., Kaufman, M., Combes, F., Baudry, A., & Bash, F. 1998, A&A, 333, 92
Brown, R. L., & Vanden Bout, P. A. 1992, ApJ, 397, L19
Carilli, C. L., Cox, P., Bertoldi, F., et al. 2002, ApJ, 575, 145
Carilli, C. L., Kohno, K., Kawabe, R., et al. 2002, AJ, 123, 1838
Carpenter, J. M., Snell, R. L., & Schloerb, F. P. 1990, ApJ, 362, 147
Dame, T. M., Hartmann, D., & Thaddeus, P. 2001, ApJ, 547, 792
Dahmen, G., Hüttemeister, S., Wilson, T. L., & Mauersberger, R. 1998, A&A331, 959
Dickman, R. L., Snell, R. L., & Schloerb, F. P. 1986, ApJ, 309, 326 (DSS86)
Evans, N. J. 1980, IAU Symp. 87, Interstellar Molecules, ed. B. H. Andrew (Dordrect: Reidel), 1
_____. 1999, ARA&A, 37, 311
Guélin, M., Zylka, R., Mezger, P. G., Haslam, C. G. T., & Kreysa, E. 1995, A&A, 298, L29
Helfer, T. T., & Blitz, L. 1997, ApJ, 478, 233
Heyer, M. H., Carpenter, J. M., & Ladd, E. F. 1996, ApJ, 463, 630
IAU Symp. 170, 1997, CO: Twenty-five Years of Millimeter-Wave Spectroscopy, eds. W. B. Latter, S. J. E. Radford, P. R. Jewell, J. G. Mangum, & J. Bally (Dordrecht: Kluwer)
Kutner, M. L. 1984, Fundamentals of Cosmic Physics, 9, 233
Langer, W. D., & Penzias, A. A. 1990, ApJ357, 477
Maddalena, R. J., Morris, M., Moscowitz, J., & Thaddeus, P. 1986, ApJ, 303, 375
Martin, H. M., Sanders, D. B., & Hill, R. E. 1984, MNRAS, 208, 35 (MSH84)

Meier, D. S., & Turner, J. L. 2001, ApJ, 551, 687
Meier, D. S., Turner, J. L., & Hurt, R. L. 2000, ApJ, 513, 200
Nagahama, T., Mizuno, A., Ogawa, H., & Fukui, Y. 1998, AJ, 116, 336
Nakai, N., & Kuno, N. 1995, PASJ, 47, 761
Plume, R., Bensch, F., Howe, J. E., et al. 2000, ApJ, 539, L133
Rand, R. J., Lord, S. D., & Higdon, J. L. 1999, ApJ, 513, 720
Rosolowski, E., Engargiola, G., Plambeck, R., & Blitz, L. 2003, ApJ, 599, 258
Sakamoto, S. 1996, ApJ, 462, 215
Sakamoto, S., Hayashi, M., Hasegawa, T., Handa, T., & Oka, T. 1994, ApJ, 425, 641
Sanders, D. B., Scoville, N. Z., & Solomon, P. M. 1985, ApJ, 289, 373
Shu, F. H. 1991, Radiation (Mill Valley: University Science Books)
Sodroski, T. J., Bennett, C., Boggess, N., et al. 1994, ApJ, 428, 638
Sodroski, T. J., Odegard, N., Dwek, E., et al. 1995, ApJ, 452, 262
Strong, A. W., Bloemen, J. B. G. M., Dame, T. M., et al. 1988, A&A, 207, 1
Strong, A. W., Moskalenko, I. V., Reimer, O., Digel, S., & Diehl, R. 2004, A&A, 422, L47
Wall, W. F. 2006, astro-ph/0601529
_____. 2006a, astro-ph/0601548
_____. 2006b, astro-ph/0601549
_____. 2006c, astro-ph, in progress
Young, J. S., & Scoville, N. Z. 1982, ApJ, 258, 467

William F. Wall: Instituto Nacional de Astrofísica, Óptica y Electrónica (INAOE), Apartados Postales 51 and 216, 72000 Puebla, Pue., México (wwall@inaoep.mx).